Research on Manual Carrier Landing Task in High Sea Conditions

XinZe Xu[1], Guanxin Hong[1] and Liang Du[2]
[1]*School of Aeronautic Science and Engineering, Beihang University, Beijing, 100191, China*
[2]*Smart Aviation Center, Hangzhou Innovation Institute of Beihang University, Hangzhou, 311115, China*

Keywords: Flight Mechanic, Pilot Model, Carrier Landing Task, Model Predictive Control, Simulation.

Abstract: A model for manual carrier-based aircraft landing missions was established for high sea condition environments. The model includes pilot, aircraft, deck motion and carrier air wake. The pilot model uses an intelligent structure, include perception, decision-making and execution modules. The perception module considers the pilot's perception of unstructured and structured data processes, established through fuzzy methods and Kalman filtering. The decision-making module is based on MPC (Model Predictive Control) methods, considering the aircraft pilot's control characteristics based on trend prediction, enabling the description of the pilot's control strategy under control input and rate constraints. The established pilot model completed flight simulations in high sea conditions. Simulation results indicate that as sea condition levels increase, the longitudinal trajectory deviation of manual landings significantly increases, with reduced correction abilities for deviations caused by ship motion, reflecting the pilot's adaptive adjustment strategy based on control resource margins under control rate and input constraints. As sea condition levels rise, the distribution of touchdown point deviations during manual landings increases, posing significant safety risks, validating that the manual landing model established in this study can be used to analyse the safety of aircraft carrier landings in complex environments.

1 INTRODUCTION

Aircraft carriers are known as the most dangerous operating airports in the world, with naval aviators being the protagonists in this hazardous operating environment. Currently, manual landing remains the primary method for aircraft carrier landings. Statistics show that 80% of accidents involving carrier-based aircraft occur during the landing process (Haitao & Yan, 2021; Wang, Jiang, Zhang, & Wen, 2022). In manual landing mode, naval aviators of carrier-based aircraft need to control three variables: speed, altitude, and lateral deviation, requiring a high level of precision in maintaining control. Providing a comprehensive description of the control behaviour of carrier-based aircraft pilots is difficult, hence practical models that satisfy the closed-loop human-machine system are typically established. Currently, there are various practical pilot models available in the field of carrier-based aircraft, categorized based on modelling principles into classical control theory models, physiology models, modern control theory models, and intelligent models (Xu, Tan, Efremov, Sun, & Qu, 2017). The classical control theory model is established based on frequency domain criteria proposed by McRuer and others. In the early days, the U.S. military often used quasi-linear models to describe the pitch channel control behaviour of pilots during the approach phase of carrier-based aircraft (D. T. McRuer & Jex, 1967). The physiology model is based on the structural pilot model proposed by Hess. Detailed explanations of this modelling approach can be found in references 5-9. These models are also based on identification results and are typically single-channel models based on classical control theory (Hess, 1980; Hess, 2006; Hess, 2019; R. A. J. P. o. t. I. o. M. E. Hess, Part G: Journal of Aerospace Engineering, 2008; M. M. Lone, Ruseno, & Cooke, 2012). With the widespread application of artificial intelligence, some scholars have also introduced intelligent methods to construct model parameters, extending this model to a wider range of flight control tasks (Brutch & Moncayo, 2024; Jakimovska, Pool, van Paassen, & Mulder, 2023).

The two types of models mentioned above mainly address the description of pilot control behavior for single-channel flight tasks (such as pitch angle tracking), but due to their inherent characteristics, they struggle to describe coupled control channel operations. NASA reports that as task complexity

Xu, X., Hong, G. and Du, L.
Research on Manual Carrier Landing Task in High Sea Conditions.
DOI: 10.5220/0013432600003970
In *Proceedings of the 15th International Conference on Simulation and Modeling Methodologies, Technologies and Applications (SIMULTECH 2025)*, pages 175-184
ISBN: 978-989-758-759-7; ISSN: 2184-2841

increases, models based on frequency domain identification results may prove insufficient (Baron, Kleinman, & Levison, 1970; Kleinman, Baron, & Levison, 1970).When it comes to multi-channel control, even if it is possible to extend the construction method of single-channel models to multiple channels, it is challenging to address the issue of model structure determination. It also requires the decoupling of each channel, which limits the application of quasi-linear models and structural models in complex conditions involving multiple inputs and multiple outputs.

Optimal pilot models based on modern control theory have significant advantages in dealing with multi-loop control problems. Since these models describe the pilot's control behavior from the perspective of overall performance based on optimal assumptions, strict decoupling is not required (Lone & Cooke, 2013; D. McRuer, Schmidt, & Dynamics, 1990). The main difference between the optimal pilot model and the structural model lies in its modeling, which is not based on frequency domain identification criteria but on an assumption that aligns with natural intuition: that human pilot control behavior is to some extent optimal. The validity of this assumption has been studied extensively (Roig, 1962). Based on experience, pilots always aim to maintain a phase margin of 50° -100° for the man-machine system. In the low frequency range, the pilot's control behavior is somewhat optimal, aligning with some theories in optimal control theory (Myers, Johnston, & McRuer, 1982). Based on the optimal assumption, discussing the pilot's control behavior from the perspective of overall performance optimization becomes feasible. By designing a reasonable model structure, the optimal model can be gradually extended to a wider range of flight tasks, such as the LQR pilot model, MOCM-AE pilot model, etc. The successful applications of these models have all demonstrated the validity of extrapolating models based on the optimal assumption (Davidson & Schmidt, 1992; Wierenga, 1969).

The ship motion induced by high sea conditions and complex ship wakes are important environmental variables affecting the safety of ship landings. A rising ship wake increases the risk of collision. Stronger ship wakes and optical guidance motions caused by heaving and pitching movements further increase tracking difficulties (optical guidance typically operates in a line-stabilized form, only able to counteract ship rotations causing motion in the optical sphere). This necessitates pilots to focus more on controlling the overall flight trends. The optimal assumption is currently the most suitable assumption for establishing a MIMO human-machine system pilot model. Therefore, this paper adopts a constrained MPC method based on the optimal assumption to establish the pilot model. Within the constraint range, this model is equivalent to the LQG pilot model, which has been proven applicable in describing pilot control behavior. At the constraint boundaries, by setting reasonable physical constraints, pilot operations align more with realworld scenarios.

The main innovation of this paper is the establishment of a pilot model for landing task, integrating the pilot's predictions and dynamic constraints during the landing process. Based on the closed-loop human-machine system established, which includes the ship motion, aircraft, pilot, and environment, research on flight safety under high sea conditions was conducted. This paper investigates the manual carrier landing task under high sea conditions. In this section, the research status of this field is elucidated. The paper describes in the second section the pilot model established based on the MPC method, and supplements necessary carrier aircraft, ship motion, and ship wake engineering models in the third section to close the human-machine system loop. Based on the established human-machine system, simulation experiments of the manual carrier landing task under high sea conditions are conducted in the fourth section, discussing the results, and summarizing the conclusions in the fifth section.

2 PILOT MODEL BASED ON MPC METHOD

2.1 Overview of Manual Landing Task

The manual landing task of carrier-based aircraft is a complex task, requiring pilots to manage variables in three channels: pitch, altitude, and lateral deviation, based on multiple perceptual information. To establish a manual landing model for high sea conditions, it is necessary to have a comprehensive understanding of carrier landing missions. This section, based on the description of carrier landing missions, constructs a conceptual manual landing model structure: the aircraft captures the desired glide slope window from a distance behind the carrier. As shown in Figure 1, guided by FLOLS, the aircraft aligns with the ideal glide path and successively completes the landing through a safety window.

Due to the movement of the carrier and the disturbance caused by the carrier's airflow wake, it is nearly impossible to maintain the flight path accurately. To minimize risks, landing signal officers are typically stationed on the carrier deck to assist pilots during landings. LSO are usually experienced pilots who guide the pilot by predicting aircraft trends for the next 2-3 seconds and ship movements. They provide verbal commands like "high" or "low" to help the pilot adjust their trajectory, which can be seen as a way of introducing future information into the guidance process.

In addition to the verbal commands from the LSO, pilots also obtain the height deviation angle Δe through the FLOLS optical guidance system during the landing process. The literature outlines the working principles of optical guidance for carrier landings (Chen, Tan, Qu, & Li, 2018). The optical guidance system provides feedback on the deviation angle between the carrier-based aircraft and the ideal glide path. There are various modelling processes involved in how pilots handle this guidance information (Chen et al., 2018; SCHMIDT, 1988). This article uses the Kalman filtering method to establish the process by which pilots convert the deviation angle Δe to height deviation ΔH as they approach the stern of the carrier. The pilots continuously self-correct based on observation results, incorporating observation noise v to simulate the pilots' observation deviation. The implementation is as follows: first, establish the state equations for optical ball displacement and height deviation. The relationship between the height deviation angle Δe, height deviation ΔH, and distance from the carrier R_x is as follows:

$$\Delta e = \frac{8}{3} * \frac{\Delta H}{R_x} \tag{1}$$

It can be observed that the value of the deviation angle is inversely proportional to the distance from the carrier. By taking $X_F = \begin{bmatrix} \frac{\Delta H}{R_x} & \frac{1}{R_x} \end{bmatrix}^T$, introducing system noise w and observation noise v, the state transition equation for the FLOLS system can be derived:

$$\begin{aligned} X(k+1) &= A_F X_F(k) + w \\ Z &= C_F X_F(k) + v \end{aligned} \tag{2}$$

The pilot's estimate of the height deviation $\Delta \hat{H}_K$ can be represented by equation (3), where F is the Kalman gain, and $\hat{X}_F$ is the estimate state of X_F:

$$\Delta \hat{H}_K = A_F \hat{X}_F(k-1) + F * \left(Z - C_F * \hat{X}_F(k)\right) \tag{3}$$

This article adopts the structure of intelligent pilot: perception, decision and execution to establish the pilot model. The manual approach landing model structure is shown in Figure 1, where G(s) represents the pilot's action execution transfer function, and the perception model is as shown in equations (1-3). The next section will establish the pilot decision model to obtain the final actual operational instruction u_p.

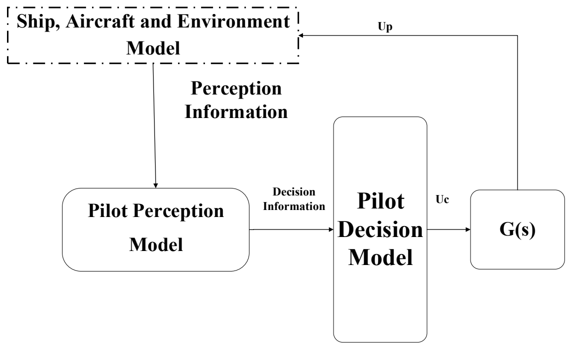

Figure 1: Perception, Decision, Action-Based Pilot Model Structure.

To make the model closely resemble the actual landing process, this article also designs the following assumptions to make the pilot model fit human capabilities to the greatest extent possible. The specific assumptions are as follows:

1. Throughout the entire process, noise generated by the pilot's own physiological characteristics is assumed to be common zero-mean white noise in nature, with noise within each time interval being independent. The intensity of the noise is linearly related to the task load.
2. The pilot will strive to make optimal decisions, but only decisions within a limited time interval will conform to the Bellman equation.
3. Regarding the dynamic characteristics of the aircraft, the pilot has sufficient prior knowledge for interpretation, and with the assistance of the landing signal officer, can roughly estimate the trend of changes in the next 2-3 seconds. The pilot will not pre-emptively act in response to unknown disturbances.
4. The sampling time for the pilot model is 0.02 seconds.

2.2 Pilot Decision Making Models Based on MPC Methods

The pilot model describes the process in which pilots make operational decisions based on the current state and future trends of the carrier-based aircraft to output the desired operational instruction u_c. Due to the need to minimize overshoot during the landing process to avoid the risk of colliding with the carrier, trend prediction has become a key focus of carrier-based aircraft pilot control techniques. Pilots are required to smoothly mesh with the carrier's movements to complete the landing, which necessitates controlling the trends in the next 2-3 seconds to counteract the optical ball fluctuations caused by the carrier's heaving motion. Considering the unique nature of carrier landing missions, this article uses prediction and optimality as two fundamental features and establishes the pilot's decision model using MPC method.

The MPC method, similar to the LQR pilot model, is based on optimal hypothesis to calculate the pilot's gains, while the LQR model is widely used to describe the pilot's control behaviour (Davidson & Schmidt, 1992). Additionally, using the MPC method can address constraint issues, which is crucial during the landing process. The following sets up a pilot model based on MPC, assuming the state space model of the controlled object as:

$$\begin{aligned} x(k+1) &= Ax(k) + Bu_c(\mathrm{k}) + Ew \\ y(k) &= Cx(k) + Du_c(k) \end{aligned} \tag{4}$$

Where：

$$\begin{aligned} x(k+P) = A^P x(k) + A^{P-1} B u_c(k) + \cdots \\ + B u_c(k+P-1) + A^P E w \end{aligned} \tag{5}$$

The recursive predictive model in Equation (5) represents the pilot's predictive behaviour regarding the flight state trends, where P is the pilot's prediction horizon, m is the control horizon, and k is the discrete step.

After establishing the mathematical model for the pilot's predictive behaviour, the next step is to establish explicit constraint equations reflecting the physical constraints the pilot faces during the carrier landing process. Constraints are common in the pilot's working environment. The residual throttle control resources left in the small perturbation model established at the conventional operating point usually range from only 10% to 15%. If hard constraints are used in modelling, it could potentially lead to divergence. Therefore, some studies describe the pilot's control behaviour as a highly constrained optimal linear controller. This significantly affects the pilot's decision behaviour, not only limiting the pilot's control performance but also introducing intelligent human characteristics based on control margins.

The advantage of the pilot model established in this paper is its ability to explicitly handle constraint issues. By introducing control constraints as performance conditions into the performance index, solving the pilot's control behaviour becomes a planning problem. The control input constraints are expressed as:

$$u_{\min(k+i)} \leq u(k+i) \leq u_{\max(k+i)} \tag{6}$$

$$\Delta U(k) \stackrel{\text{def}}{=} \begin{bmatrix} \Delta u(k) \\ \Delta u(k+1) \\ \vdots \\ \Delta u(k+m-1) \end{bmatrix} \tag{7}$$

$$\Delta Y_p(k) \stackrel{\text{def}}{=} \begin{bmatrix} \Delta y_p(k+1|k) \\ \Delta y_p(k+2|k) \\ \vdots \\ \Delta y_p(k+p|k) \end{bmatrix} \tag{8}$$

Clearly, the objective function J contains inequalities, making it impossible to obtain an analytically optimal pilot gain solution through solving the Riccati equation. This is a typical Quadratic Programming (QP) problem. Based on Assumption 2, it is assumed that the pilot will optimize the performance function at each sampling instant.

Physically, the optimal gain represents the pilot's control strategy that minimizes the overall deviation of the flight state through a combination of experience and the pilot's estimation of the flight trends. By selecting appropriate Q and R values, inhuman control behaviour can be avoided, typically requiring state variables other than altitude and lateral position not to exceed 1. QP problems are a classic type of optimization problem for which mature numerical optimization methods exist, making them well-studied problems. Therefore, transforming the pilot's decision problem into the standard form of a QP problem allows for its solution. The standard form of a QP problem is:

$$\min_{z} z^T H z - g^T z \text{, Where } Cz \geq b \tag{9}$$

To standardize the predictive equation as in Equation (8), we have:

$$\begin{aligned} z &= U(k) \\ H &= S_u^T Q^T Q S_u + R^T R \\ G(k+1|k) &= 2 S_u^T Q^T Q E(k+1|k) \end{aligned} \tag{10}$$

Therefore, the objective function transforms into:

$$\tilde{J} = \Delta U(k)^T H \Delta U(k) - G(k+1|k)^T \Delta U(k) \tag{11}$$

Where：

$$E(k+1) = R(k+1) - S_x\Delta x(k) - Iy_c(k) - S_d\Delta$$

$$S_x = \begin{bmatrix} CA \\ \sum_i^2 CA^i \\ \vdots \\ \sum_i^p CA^i \end{bmatrix},\ I = \begin{bmatrix} I_{n\times n} \\ I_{n\times n} \\ \vdots \\ I_{n\times n} \end{bmatrix},\ S_d = \begin{bmatrix} CB \\ \sum_i^2 CA^{i-1}B \\ \vdots \\ \sum_i^p CA^{i-1}B \end{bmatrix}$$

$$S_u = \begin{bmatrix} CB & 0 & 0 & \dots & 0 \\ \sum_i^2 CA^{i-1}B & CB & 0 & \dots & 0 \\ \vdots & \vdots & \vdots & \ddots & \vdots \\ \sum_i^m CA^{i-1}B & \sum_i^{m-1} CA^{i-1}B & \dots & \dots & CB \\ \vdots & \vdots & \vdots & \ddots & \vdots \\ \sum_i^p CA^{i-1}B & \sum_i^{p-1} CA^{i-1}B & \dots & \dots & \sum_i^{p-m+1} CA^{i-1}B \end{bmatrix} \tag{12}$$

Although physical plant constraints are constant, in the model above, control constraints depend on the control margin at the current sampling instant. Therefore, the constraints are time varying. For any arbitrary time t_0, after discretization, we have:

$$\Delta u_{\max(k)} = u_{\max(k)} - u(k)$$

$$\Delta U_{\max(k)} \overset{\text{def}}{=} \begin{bmatrix} u_{\max(k)} - u(k-1) \\ u_{\max(k)} - u(k) \\ \vdots \\ u_{\max(k)} - u(k+m-1) \end{bmatrix} \tag{13}$$

Therefore, by considering the form of ΔU(k), the inequality structure can be obtained as:

$$\begin{bmatrix} -I \\ I \end{bmatrix} \Delta U(k) \geq \Delta U_{max}(k) \tag{14}$$

Consequently, we have transformed the pilot's decision problem into the standard form of a QP problem. Numerical optimization methods for QP problems are well established, such as interior point methods, which can be used for solving. I will not delve into details here. Once we obtain the pilot gain K_{pilot}, we will have established a complete decision-making model to derive the pilot's desired command u_c .In conclusion, the overall structure of the pilot model with constraints added is illustrated in Figure 2.

3 AIRCRAFT SYSTEM

3.1 Aircraft System Model

To study the artificial landing model of carrier-based aircraft in high sea conditions, it is necessary to establish a model of the carrier-based aircraft. The dynamic characteristics of the carrier-based aircraft model will significantly impact the pilot's landing performance. In landing tasks, the aerodynamic effects of the carrier-based aircraft generally satisfy the assumption of small disturbances, thus a linear system is used to establish the model of the carrier-based aircraft (Sweger, 2003). The dynamic equation is as follows

$$\begin{aligned} \dot{x} &= Ax + Bu + Ew \\ y &= Cx + Du_p \end{aligned} \tag{15}$$

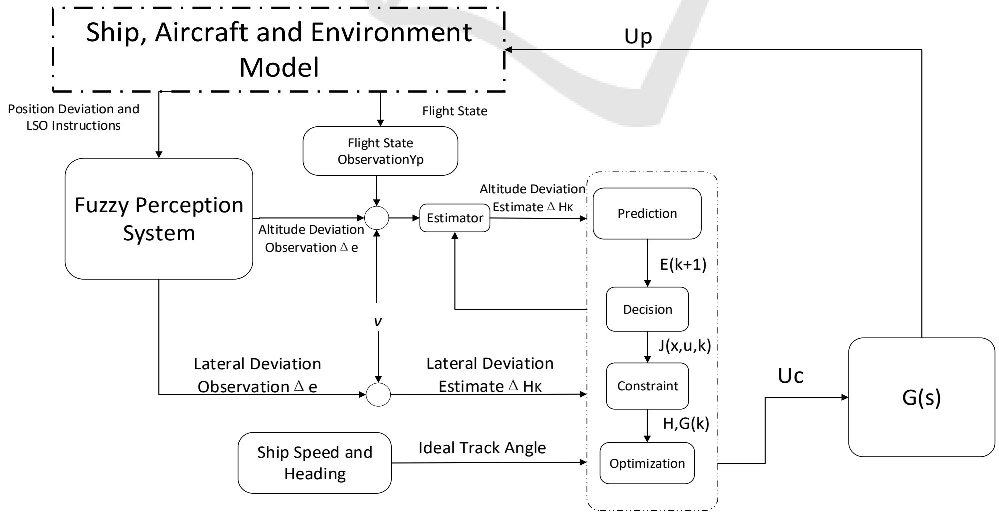

Figure 2: The Overall Structure of Constrained Predictive Pilot Model.

Where the state variable x is:

$$x = [X, Y, Z, \phi, \theta, \varphi, V, \alpha, \beta, p, q, r]$$

In the state vector, X, Y, Z represent the displacements of the carrier-based aircraft in the earth fixed reference frame, ϕ, θ, φ are the three Euler angles of the aircraft, V, α, β denote the airspeed, angle of attack, and sideslip angle of the aircraft, and p, q, r are the three Euler angular velocities of the aircraft.

The control input u is:

$$u = [\delta_e, \delta_a, \delta_r, \delta_t]$$

In the control vector, δ_e represents the elevator deflection command, δ_a is the aileron deflection command, δ_r is the rudder deflection command, and δ_t is the throttle command.

The inner-loop control structure of the aircraft system is shown in figure 3, aiming to enhance the flight quality of the system through feedback of α and q (Chen et al., 2018). Due to the use of pure gain feedback, the system matrix containing stability augmentation control can be obtained through linear transformation. The control model used in this paper has been somewhat simplified, incorporating the effects of elevator surfaces and throttle as control rate constraints into the pilot model. This is done to analyze the impact of throttle delays and elevator rate limits on control performance.

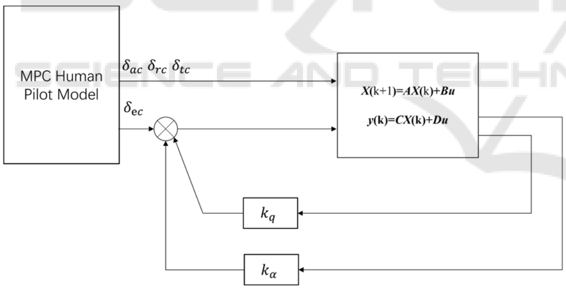

Figure 3: Block diagram of the aircraft system.

3.2 Carrier Desire Target Point Model

The position offset of the aircraft is calculated based on the ideal glide path, with the origin of the ideal glide path located above the aircraft carrier deck. Therefore, it is influenced by both the translational and angular displacements of the ship. In high sea conditions, the ship will experience more intense motion, which is a crucial factor affecting landing safety. Hence, to analyse the impact of high sea conditions on manual landings, it is necessary to establish a ship motion model.

The ship motion model in this paper utilizes the ISSC double parameter spectrum to calculate wave disturbances, deriving wave interference forces. Based on the ship's state space response, the time history curve of ship motion is obtained. The ship state space is defined as:

$$\dot{x}_S = A_s x_s + B_s u_w \tag{16}$$

The state variable x_s represents:

$$x_s = [X, Y, Z, \phi_s, \theta_s, \varphi_s, u_s, v_s, w_s, p_s, q_s, r_s]$$

The control input u_w represents the wave disturbance force. After obtaining the ship motion, the ideal landing point velocity can be derived, as shown in the following equation:

$$\begin{cases} u_{DTP} = V_s cos\varphi_s \\ v_{DTP} = V_s \sin(-\psi_{AD})\, sin\varphi_s \\ w_{DTP} = w_s + V_s(sin\theta_s - sin\phi_s cos\theta_s + cos\theta_s cos\phi_s) \end{cases} \tag{17}$$

u_{DTP}、v_{DTP}、w_{DTP} are the three axis velocities of the desired touchdown point in the landing coordinate system, V_s is the speed of the ship, and ψ_{AD} is the deck angle.

3.3 Carrier Air Wake Model

In high sea conditions, due to the more intense ship motion and environmental winds, the disturbance intensity of the ship's wake will also increase accordingly. The ship's wake consists of four components, and in the landing coordinate system, the three axis ship wake field is as follows(Peng, Jin, & ASTRONAUTICS, 2000):

$$\begin{cases} u_w = u_1 + u_2 + u_3 + u_4 \\ v_w = v_1 + v_4 \\ w_w = w_1 + w_2 + w_3 + w_4 \end{cases} \tag{18}$$

In the equation, u_1、v_1、w_1 represent random free atmospheric turbulence components. u_2、w_2 represent steady components of the ship's wake. u_3、w_3 represent periodic components of the ship's wake. u_4、v_4、w_4 represent random components of the ship's wake.

4 SIMULATION

In the preceding sections, models for carrier-based aircraft, ship motion, environmental wind, and pilot behaviour were established. This paper focuses on sea conditions 4, 5, and 6 as the research subjects. The methods for calculating ship wakes and ship motion are provided in Section 3. Simulation results are shown in Figure 4. The results indicate that as the sea condition level increases, the ship's wake motion increases with the sea condition level, and the corresponding vertical disturbances of the ship's wake flow are enhanced. Even under sea condition 6 conditions, the ship's wake motion remains less than ±1.7m, which aligns with the operational conditions of carrier-based aircraft in the literature. Therefore, the simulated conditions in this paper are considered reasonable.

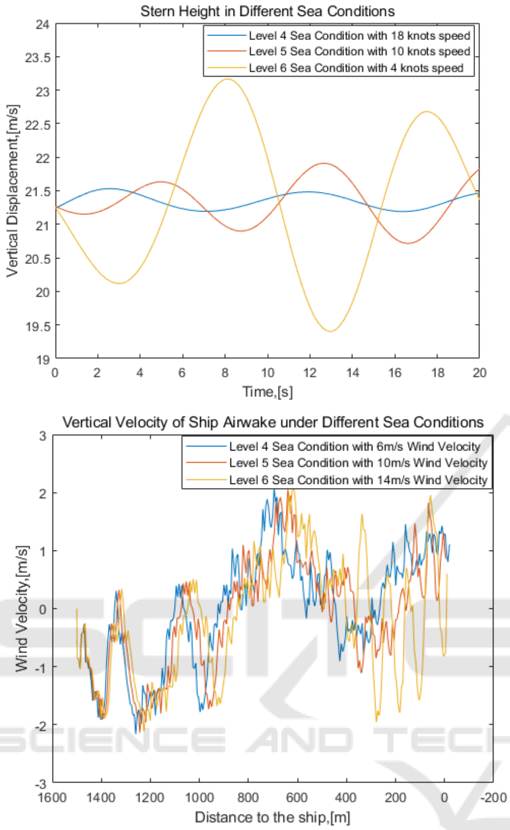

Figure 4: Ship motion and air wake in Level 4-6 sea condition.

The above environmental conditions serve as inputs to the simulated study of arrested landings in high sea conditions. The parameters for the pilot model are specified in Table 1:

Table 1: Pilot Model Parameters.

	Control Constraints					Weight Matrix	
Para-meter	Input	δ_e	δ_a	δ_r	δ_t	State	Control
	Upper Bound	10.5	25	1	90	Q_y	R_u
	Lower Bound	-25	-25	-3	75		
	Vehicle	5	5	0.1	0.1		

Conducting simulated arrested landings in high sea conditions according to the parameters in Table 1, Figure 5 depicts the behavioural characterization

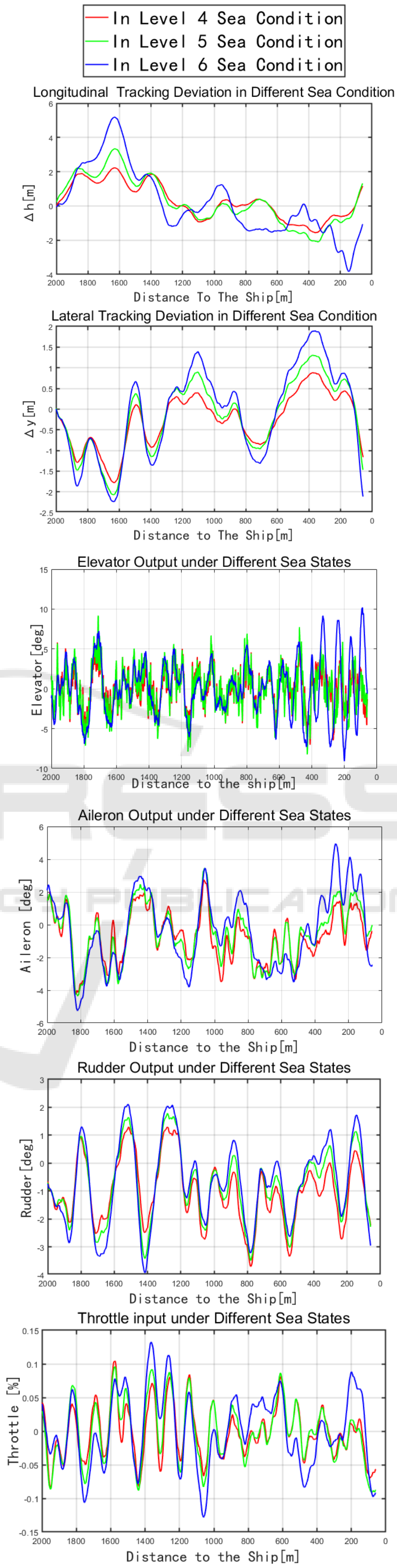

Figure 5: Pilot Model Output in Level 4,5,6 Sea Conditions.

of pilots in high sea conditions. The simulation results indicate that the pilot's control magnitude increases in sea conditions 4, 5, and 6. In sea condition 6, the ship's wake significantly affects the pilot's landing operations, showing a trend of oscillation at the ship's wake, with a notable increase in nonlinear components in the control command output.

To further conduct a safety analysis of carrier landings in high sea conditions, repeated simulation experiments are carried out to study the statistical characteristics and safety features of arrested landings in high sea conditions. The repeated simulation conditions are outlined in Table 2.

Figure 6 displays box plots of the deviations of three landing elements in sea conditions 4, 5, and 6. These elements include altitude deviation, lateral deviation, and pitch angle deviation, which are the three main control quantities that pilots need to focus on during landing tasks. The box plot is a statistical chart used to display the distribution of data. In box plot, the data is divided into five parts: the upper whisker, upper quartile, median, lower quartile, and lower whisker. The upper whisker represents the maximum value of the data, while the lower whisker represents the minimum value. The line in the middle of the box represents the median (the 50th percentile), and there are horizontal lines at the top and bottom of the box representing the upper quartile and lower quartile, respectively. Box plots also include the display of outliers, which are values that are typically far from most data points. Box plots provide a clear visualization of the data's spread, median, quartiles, and the distribution of outliers.

Table 2: Simulation Conditions for High Sea condition Deck Landing.

Name	Work Condition	Unit
Sea conditions	4, 5, 6	/
Wind of deck	25	kn
Average wind speed	6, 8, 14	m/s
Aircraft speed	62	m/s
γ	-4	°
Number of Repetitions	45	/

The results indicate that as the sea condition level increases, the longitudinal deviation in arrested landings gradually increases. The variance of lateral deviation remains approximately constant, but the distribution leans more towards the right side of the ship's wake. This is because pilots have lower tolerance for deviations in the longitudinal channel, prioritizing corrections in that direction. This, coupled with the longitudinal-lateral coupling, affects corrections towards the centre, resulting in insufficient correction for lateral deviations induced by carrier motion.

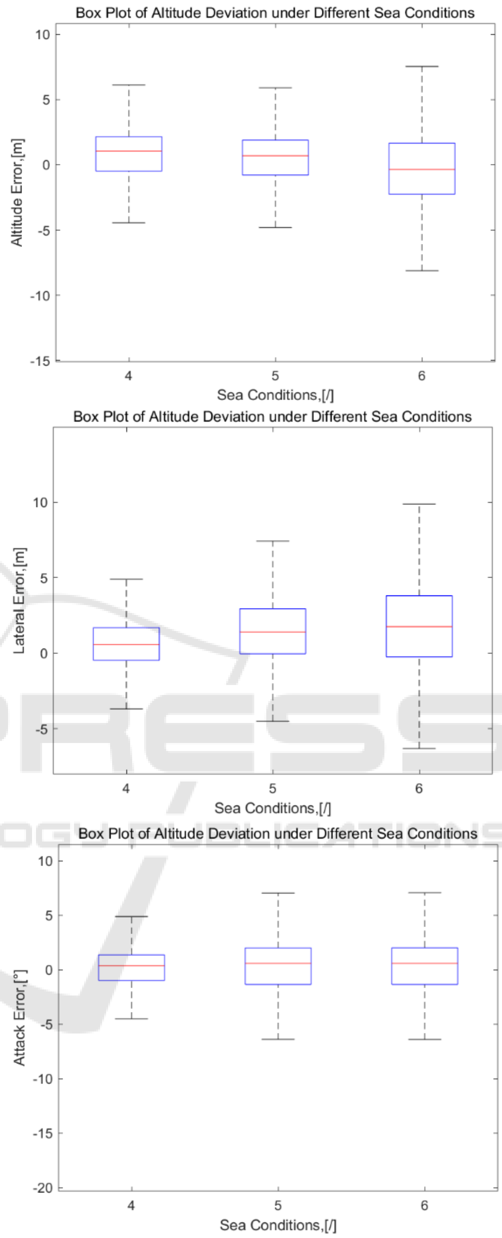

Figure 6: Box plot of landing three elements' deviations in sea condition 4-6.

Figure 7 shows the hook-to-ramp (The vertical distance between the hook and the ramp when the aircraft passes through the ramp) clearance of aircraft passing over the ship's wake in sea conditions 4, 5, and 6. The hook-to-ramp clearance represents the safety margin during arrested landings, typically requiring at least a 4-meter hook-to-ramp distance for safety. It can be observed that in sea condition 4, manual arrested landings can ensure a hook-to-ramp distance of at least 4 meters, descending from a position slightly above the ideal trajectory towards the ship's wake, as described in the literature. In sea condition 5, the dispersion of hook-to-ramp distances increases, with a tendency to cross the 4-meter safety line. In sea condition 6, pilots struggle to maintain a safe margin of 4 meters for the hook-to-ramp distance, posing significant safety risks during arrested landings.

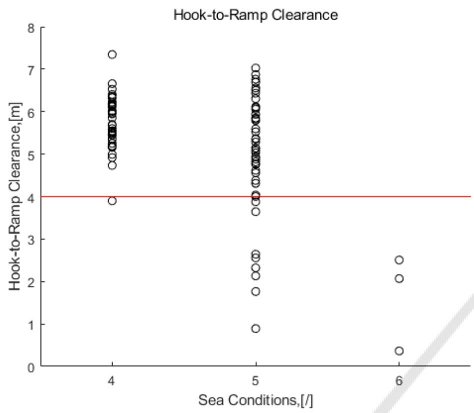

Figure 7: Hook-to-ramp clearance of carrier-based aircraft in sea conditions 4-6.

5 CONCLUSIONS

This article addresses the modelling issues of carrier landings task in high sea conditions by establishing models that include a carrier-based aircraft model, deck motion model, carrier air wake model, and pilot model, taking into account the pilot's perception and decision-making processes. The main conclusions are as follows:

1. The pilot models based on MPC method under optimal assumptions, representing a MIMO pilot model that controls based on the overall state of the human-machine system. Compared to the LQR pilot model, the MPC pilot model can describe the flight techniques where pilots control based on the trend changes of the ship's movement and has the structural advantage of explicitly handling constraints.
2. Simulation results indicate that in high sea conditions, the longitudinal deviation during manual arrested landings increases. Due to pilots' low tolerance for longitudinal deviations and their high correction priority, corrections for lateral deviations induced by ship motion are insufficient, leading to an overall right leaning lateral deviation. The simulations also demonstrate that as sea condition levels rise, the dispersion of hook-to-ramp distances increases with a tendency to exceed the 4-meter safety line, posing significant safety risks. This confirms that the model proposed in this study can be used for safety analysis of manual carrier landing task in complex environments.

REFERENCES

Baron, S., Kleinman, D. L., & Levison, W. H. (1970). An optimal control model of human response part II: Prediction of human performance in a complex task. *Automatica, 6*(3), 371-383. doi:https://doi.org/10.1016/0005-1098(70)90052-X

Brictson, C. A. (1966). *Measures of pilot performance: Comparative analysis of day and night carrier recoveries*: University of Southern California.

Brutch, S., & Moncayo, H. (2024). *Machine Learning Approach to Estimation of Human-Pilot Model Parameters.* Paper presented at the AIAA SCITECH 2024 Forum.

Chen, C., Tan, W., Qu, X., & Li, H. (2018). A Fuzzy Human Pilot Model of Longitudinal Control for a Carrier Landing Task. *IEEE Transactions on Aerospace and Electronic Systems, 54*(1), 453-466. doi:10.1109/TAES.2017.2760779

Davidson, J. B., & Schmidt, D. K. (1992). *Modified optimal control pilot model for compute r-aided design and analysis*. Retrieved from

Haitao, Y., & Yan, L. (2021, 19-22 Nov. 2021). *Research on Key Technologies of Carrier-Based Aircraft Landing.* Paper presented at the 2021 6th International Conference on Robotics and Automation Engineering (ICRAE).

Hess, R. A. (1980). Structural Model of the Adaptive Human Pilot. *Journal of Guidance and Control, 3*(5), 416-423. doi:10.2514/3.56015

Hess, R. A. (2006). Simplified approach for modelling pilot pursuit control behaviour in multi-loop flight control tasks. *Proceedings of the Institution of Mechanical Engineers, Part G: Journal of Aerospace Engineering, 220*(2), 85-102.

Hess, R. A. (2019). Analysis of the Aircraft Carrier Landing Task, Pilot + Augmentation/Automation. *IFAC-PapersOnLine, 51*(34), 359-365. doi:https://doi.org/10.1016/j.ifacol.2019.01.017

Hess, R. A. J. P. o. t. I. o. M. E., Part G: Journal of Aerospace Engineering. (2008). Obtaining multi-loop pursuit-control pilot models from computer simulation. *222*(2), 189-199.

Jakimovska, N., Pool, D. M., van Paassen, M. M., & Mulder, M. (2023). *Using the Hess Adaptive Pilot Model for Modeling Human Operator's Control Adaptations in Pursuit Tracking.* Paper presented at the AIAA SCITECH 2023 Forum.

Kleinman, D. L., Baron, S., & Levison, W. H. (1970). An optimal control model of human response part I: Theory and validation. *Automatica, 6*(3), 357-369. doi:https://doi.org/10.1016/0005-1098(70)90051-8

Lone, M. M., & Cooke, A. K. J. P. o. t. I. o. M. E., Part G: Journal of aerospace engineering. (2013). Pilot-model-in-the-loop simulation environment to study large aircraft dynamics. *227*(3), 555-568.

Lone, M. M., Ruseno, N., & Cooke, A. K. (2012). Towards understanding effects of non-linear flight control system elements on inexperienced pilots. *The Aeronautical Journal (1968), 116*(1185), 1201-1206. doi:10.1017/S0001924000007569

McRuer, D., Schmidt, D. K. J. J. o. G., Control,, & Dynamics. (1990). Pilot-vehicle analysis of multiaxis tasks. *13*(2), 348-355.

McRuer, D. T., & Jex, H. R. (1967). A Review of Quasi-Linear Pilot Models. *IEEE Transactions on Human Factors in Electronics, HFE-8*(3), 231-249. doi:10.1109/THFE.1967.234304

Myers, T. T., Johnston, D. E., & McRuer, D. J. N. C.-., June. (1982). Space shuttle flying qualities and flight control system assessment study.

Peng, J., Jin, C.-j. J. J.-B. U. O. A., & ASTRONAUTICS. (2000). Research on the numerical simulation of aircraft carrier air wake. *26*(3; ISSU 103), 340-343.

Roig, R. W. (1962). A comparison between human operator and optimum linear controller RMS-error performance. *IRE Transactions on human factors in electronics*(1), 18-21.

SCHMIDT, D. (1988). *Modeling human perception and estimation of kinematic responses during aircraft landing.* Paper presented at the Guidance, Navigation and Control Conference.

Sweger, J. F. (2003). *Design specifications development for unmanned aircraft carrier landings: A simulation approach*: US Naval Academy.

Wang, L., Jiang, X., Zhang, Z., & Wen, Z. (2022). Lateral automatic landing guidance law based on risk-state model predictive control. *ISA Transactions, 128*, 611-623. doi:https://doi.org/10.1016/j.isatra.2021.11.031

Wierenga, R. D. J. I. T. o. M.-M. S. (1969). An evaluation of a pilot model based on Kalman filtering and optimal control. *10*(4), 108-117.

Xu, S. T., Tan, W. Q., Efremov, A. V., Sun, L. G., & Qu, X. J. (2017). Review of control models for human pilot behavior. *Annual Reviews in Control, 44*, 274-291. doi:10.1016/j.arcontrol.2017.09.009.